



UvA-DARE (Digital Academic Repository)

Optimization of adaptive radiation therapy in cervical cancer: Solutions for photon and proton therapy

van de Schoot, A.J.A.J.

Publication date

2016

Document Version

Final published version

[Link to publication](#)

Citation for published version (APA):

van de Schoot, A. J. A. J. (2016). *Optimization of adaptive radiation therapy in cervical cancer: Solutions for photon and proton therapy*. [Thesis, fully internal, Universiteit van Amsterdam].

General rights

It is not permitted to download or to forward/distribute the text or part of it without the consent of the author(s) and/or copyright holder(s), other than for strictly personal, individual use, unless the work is under an open content license (like Creative Commons).

Disclaimer/Complaints regulations

If you believe that digital publication of certain material infringes any of your rights or (privacy) interests, please let the Library know, stating your reasons. In case of a legitimate complaint, the Library will make the material inaccessible and/or remove it from the website. Please Ask the Library: <https://uba.uva.nl/en/contact>, or a letter to: Library of the University of Amsterdam, Secretariat, P.O. Box 19185, 1000 GD Amsterdam, The Netherlands. You will be contacted as soon as possible.

Chapter 5

Dosimetric advantages of proton therapy compared with photon therapy using an adaptive strategy in cervical cancer

A version of this chapter has been published as:

Dosimetric advantages of proton therapy compared with photon therapy using an adaptive strategy in cervical cancer

A.J.A.J. van de Schoot, P. de Boer, K.F. Crama, J. Visser, L.J.A. Stalpers,
C.R.N. Rasch and A. Bel

Acta Oncologica 2016; DOI:10.3109/0284186X.2016.1139179.

<http://dx.doi.org/10.3109/0284186X.2016.1139179>

Abstract

Purpose

Image-guided adaptive proton therapy (IGAPT) can potentially be applied to take into account interfraction motion while limiting organ at risk (OAR) dose in cervical cancer radiation therapy (RT). In this study, the potential dosimetric advantages of IGAPT compared with photon-based image-guided adaptive RT (IGART) were investigated.

Material & Methods

For thirteen cervical cancer patients, full and empty bladder planning computed tomography (CT) images and weekly CTs were acquired. Based on both primary clinical target volumes (pCTVs) (i.e. gross tumor volume (GTV), cervix, corpus-uterus and upper part of the vagina) on planning CTs, the pre-treatment observed full-range primary internal target volume (pITV) was interpolated to derive pITV subranges. Given corresponding ITVs (i.e. pITVs including lymph nodes), patient-specific photon and proton plan libraries were generated. Using all weekly CTs, IGART and IGAPT treatments were simulated by selecting library plans and recalculating the dose. For each recalculated IGART and IGAPT fraction, CTV (i.e. pCTV including lymph nodes) coverage was assessed and differences in fractionated substitutes of dose-volume histogram (DVH) parameters (V_{15Gy} , V_{30Gy} , V_{45Gy} , D_{mean} , D_{2cc}) for bladder, bowel and rectum were tested for significance (Wilcoxon signed-rank test). Also, differences in toxicity-related DVH parameters (rectum V_{30Gy} , bowel V_{45Gy}) were approximated based on accumulated dose distributions.

Results

In 92% (96%) of all recalculated IGAPT (IGART) fractions adequate CTV coverage ($V_{95\%} > 98\%$) was obtained. All dose parameters for bladder, bowel and rectum, except the fractionated substitute for rectum V_{45Gy} , were improved using IGAPT. Also, IGAPT reduced the mean dose to bowel, bladder and rectum significantly ($p < 0.01$). In addition, an average decrease of rectum V_{30Gy} and bowel V_{45Gy} indicated reductions in toxicity probabilities when using IGAPT.

Conclusion

This study demonstrates the feasibility of IGAPT in cervical cancer using a plan-library based plan-of-the-day approach. Compared to photon-based IGART, IGAPT maintains target coverage while significant dose reductions for the bladder, bowel and rectum can be achieved.

5.1 | Introduction

Radiation therapy (RT) for patients with locally advanced cervical cancer usually consists of external beam RT (EBRT) with concomitant chemotherapy or hyperthermia and subsequently brachytherapy [72]. Compared to conformal EBRT, intensity-modulated RT (IMRT) allows highly conformal dose distributions resulting in decreased organ at risk (OAR) dose [119]. To completely benefit from this potential advantage, adequate patient set-up based on daily image guidance is essential. However, despite drinking instructions, large bladder volume variations may induce interfraction target motion which increases the risk of target under-dosing and limits OAR sparing [73].

Pre-fraction cone-beam CT (CBCT) allows adapting the radiation delivery during the course of treatment. This is known as adaptive RT (ART) and several ART strategies have been investigated [53,56]. Similar to our current clinical practice, a practical approach frequently applied for pelvic EBRT is the plan-library based plan-of-the-day strategy [58,59]. Based on the pre-treatment acquired target motion range, treatment plans corresponding to different target shapes and positions are created and using pre-fraction CBCT the plan best fitting the target shape is selected. Also in cervical cancer, this online adaptive strategy has the potential to correct for most interfraction target motion to ensure daily target coverage. However, OARs still receive substantial dose during photon-based image-guided ART (IGART) [58,59].

Compared to photons, protons have certain distinct advantages due to their finite range and hold the promise of limited OAR toxicity [34,69]. Intensity-modulated proton therapy (IMPT) enables a highly conformal dose delivery to complex-shaped target volumes including steep dose fall-offs around the target. However, due to its sensitivity to range and position uncertainties, IMPT dose delivery requires appropriate online image guidance [24]. Moreover, anatomical changes can largely influence dose delivery and therefore IMPT can benefit from treatment adaptation based on pre-fraction imaging.

Previously, only a limited number of studies investigated the potential benefit of proton-based RT compared to photon-based RT in cervical cancer [69-71,123]. Even though the planning target volume (PTV) concept is less suitable for IMPT [24], those studies used the PTV concept to anticipate on uncertainties. Moreover, none of them recalculated planned dose distributions using additional imaging data in order to evaluate differences between photon-based and proton-based RT in terms of delivered dose.

To investigate the actual benefit of proton therapy in cervical cancer, differences in delivered dose between photon-based and proton-based RT treatments using an adaptive strategy need to be determined. Therefore, our aim was to investigate the dosimetric advantages of image-guided adaptive proton therapy (IGAPT) in cervical cancer compared to photon-based IGART. Using a plan-library based plan-of-the-day adaptive strategy, both IGAPT and IGART treatments were simulated by recalculating selected plans on weekly CTs. Differences were evaluated in terms of dose-volume histogram (DVH) parameters and normal tissue complication probability (NTCP).

5.2 | Material & Methods

Patients and imaging

Thirteen cervical cancer patients treated with photon-based RT between January 2014 and August 2015 were included after obtaining written informed consent for additional CT imaging. These additional CTs were acquired solely for a pilot study to explore the potential benefit of ART and were approved by the local medical ethical committee. One patient was excluded because of image artifacts induced by a metal hip prosthesis. Patients were treated in prone position using a belly board device and in supine position when selected for para-aortic irradiation or when the prone position was not possible. In order to treat with a full bladder, patients were instructed to empty their bladder, to drink 0.5 liter of water, and to refrain from voiding 1.5 h prior to irradiation. Table 5.1 presents patient characteristics and clinical treatment details.

Besides the full bladder planning CT, an additional empty bladder planning CT prior to treatment and weekly CTs directly after RT delivery were acquired. All CT images with a slice thickness of 2.5 mm were obtained in RT treatment position. For two patients, the empty bladder planning CT was not acquired and the weekly CT with the smallest bladder volume was used as surrogate and excluded for treatment simulations. Three patients received four instead of five weekly CTs due to logistical issues and one patient received an additional sixth CT due to clinical issues regarding tumor response. The radiation oncologist delineated on all CTs the gross tumor volume (GTV), corpus-uterus, cervix, upper part of the vagina and elective lymph nodes. Also, the body, bowel cavity, as a surrogate for small bowel, rectum, kidneys and bladder were delineated using Radiation Therapy Oncology Group (RTOG) guidelines [137]. The primary CTV (pCTV) encompasses the GTV, cervix, corpus-uterus and upper part of the vagina. The CTV included the pCTV and elective lymph nodes.

Library of structures

After bony registration of both planning CTs, the pCTV on the full bladder planning CT was registered to the pCTV on the empty bladder planning CT using a structure-based deformable image registration algorithm [78]. The obtained deformation vectors after registration represented the connection between corresponding points on both structures. By linear scaling of the deformation vectors, the patient-specific full-range primary internal target volume (pITV) was divided into three, one or two pITV subranges when the corpus-uterus tip displacement was above 20 mm, below 10 mm or in between, respectively (Table 5.1, Figure 5.1). Corresponding to each pITV subrange an ITV was constructed by including elective lymph nodes.

Table 5.1 | Patient characteristics.

Patient	FIGO stage	Type of irradiation	Fractionation scheme	Clinical treatment		Treatment position	No. of CTs (repeat CTs)	No. of ITVs	
1	*	IB2	pelvic	23 x 2.0 Gy	5-field IMRT	non-ART	prone	6 (4)	1
2	**	IIB	pelvic	23 x 2.0 Gy	dual-arc VMAT	non-ART	prone	7 (5)	3
3	*	IB2	pelvic	23 x 2.0 Gy	dual-arc VMAT	non-ART	prone	8 (6)	3
4	**	IIA	pelvic	23 x 2.0 Gy	5-field IMRT	non-ART	prone	7 (5)	3
5	**	IIB	pelvic	23 x 2.0 Gy	5-field IMRT	non-ART	supine	6 (5)	3
6	*	IIA	pelvic	23 x 2.0 Gy	dual-arc VMAT	non-ART	prone	7 (5)	2
7	*	IIB	para-aortic	28 x 1.8 Gy	dual-arc VMAT	non-ART	supine	7 (5)	1
8	**	IIB	pelvic	23 x 2.0 Gy	dual-arc VMAT	non-ART	prone	5 (4)	3
9	*	IIIB	para-aortic	28 x 1.8 Gy	dual-arc VMAT	non-ART	supine	7 (5)	2
10	**	IIB	pelvic	23 x 2.0 Gy	dual-arc VMAT	non-ART	supine	7 (5)	3
11	*	IB1	pelvic	23 x 2.0 Gy	dual-arc VMAT	ART	supine	7 (5)	2
12	*	IB1	pelvic	23 x 2.0 Gy	dual-arc VMAT	ART	supine	6 (4)	3

Abbreviations: FIGO = International Federation of Gynecology and Obstetrics; CT = computed tomography; ITV = internal target volume; ART = adaptive radiation therapy; VMAT = volumetric modulated arc therapy; IMRT = intensity modulated radiation therapy.

* All CTs acquired with LightSpeed RT16, General Electric Company, Waukesha WI, USA.

** All CTs acquired with LightSpeed RT16, General Electric Company, Waukesha WI, USA. Only full bladder planning CT acquired with Gemini TF, Philips Medical Systems, Eindhoven, the Netherlands.

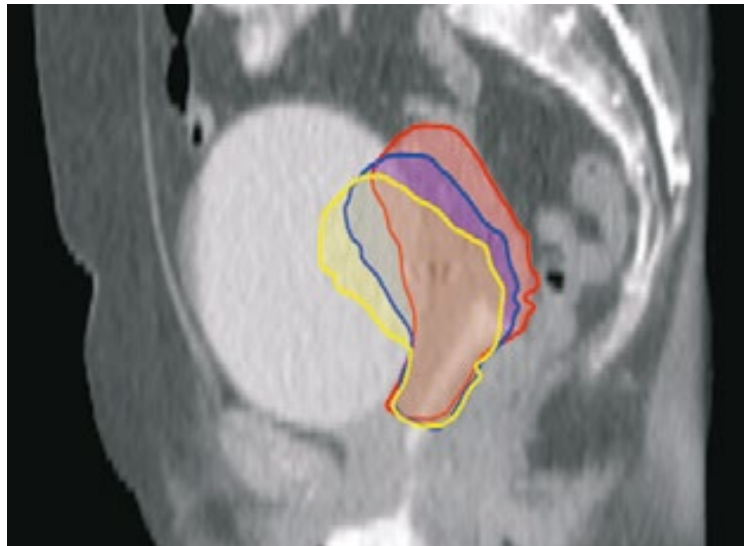


Figure 5.1 | Sagittal view of the full bladder planning CT for a patient that showed large cervix-uterus motion (corpus-uterus tip displacement >2.0 cm) induced by bladder volume variation. The three illustrated primary ITV subranges (red, blue and yellow) are obtained by dividing the full-range primary ITV based on linear scaling of the obtained deformation vectors.

Treatment planning

All treatment plans were generated with RayStation (version 4.4, RaySearch Laboratories AB, Stockholm, Sweden). Contrast agent induced high-density values on planning CTs used for vagina or bowel and bladder visualization were corrected to muscle (1.05 g/cm^3) and water (1.0 g/cm^3) density, respectively. Patient-specific plan libraries for both photons and protons were created based on a prescribed physical ITV dose of 46 Gy ($23 \times 2 \text{ Gy}$) for pelvic irradiation or 50.4 Gy ($28 \times 1.8 \text{ Gy}$) for para-aortic irradiation. Plans were robustly optimized on a uniform 3 mm dose grid with the beam isocenter set to the ITV center of mass using the full bladder planning CT [129]. Plan optimizations were started with the initial set of planning objectives for each plan (Table 5.2) and objective values were individually optimized to minimize OAR dose while maintaining International Commission on Radiation Units & Measurements (ICRU) based ITV coverage ($D_{98\%} > 95\%$, $D_{2\%} < 107\%$). Since the prescribed target dose is below OAR dose limits, only target coverage robustness was evaluated by applying errors and recalculating the dose. For all perturbed dose distributions adequate ITV coverage was required.

Photon plans were generated using a 10-MV dual-arc volumetric modulated arc therapy (VMAT) technique (356° per arc, fixed 20° collimator angle). Besides the nominal isocenter position, six isocenter position shifts in each main direction (left, right, inferior, superior, posterior, anterior) were included to consider in total seven scenarios for robust optimization. Position shifts of 8 mm were applied, which equals the clinically used ITV-to-PTV margin in cervical cancer RT. For robustness evaluation, next to the six error scenarios used for optimization, eight additional error scenarios with 8 mm isocenter shifts along the diagonal of each octant in three-dimensional space were added. In total, 14 error scenarios were considered for ITV coverage robustness evaluation.

Table 5.2 | Initial set of planning objectives used for pelvic (para-aortic) irradiation. An asterisk indicates planning objectives only used for para-aortic irradiation.

Planning objectives		
CTV	Minimum dose 46 (50.40) Gy	w=120
	Maximum dose 46.80 (51.40) Gy	w=80
Body	Dose fall-off: 46–30 (51.40–36) Gy over 1.20 cm	w=50
Rectum	Maximum dose 43.70 (47.88) Gy	w=10
	Maximum 30 Gy to 70% (80%) of the volume	w=5
Bladder	Maximum dose 43.70 (47.88) Gy	w=10
	Maximum 30 Gy to 70% (80%) of the volume	w=5
Bowel cavity	Maximum dose 43.70 (47.88) Gy	w=10
Kidney	* Maximum 18 Gy to 33% of the volume	w=25

Abbreviations: CTV = clinical target volume; w = weight.

IMPT plans were generated based on pencil beam scanning (spot size in air: $\sigma=2.5$ mm – 7.0 mm (226.7 MeV – 70.0 MeV)) using four fixed posterior beams (30°, 90°, 270°, 330° (prone); 90°, 150°, 210°, 270° (supine)) [138]. Assuming a proton relative biological effectiveness of 1.1 [139], IMPT plans were created with a prescribed ITV dose of 46 Gy-equivalent or 50.4 Gy-equivalent. Besides the nominal isocenter position and the six isocenter position shifts of 8 mm in the main directions also three range errors (3%, 0%, -3%) were included to consider in total 21 scenarios for robust optimization. ITV coverage robustness was evaluated using 28 error scenarios, consisting of 14 position errors (8 mm) and 2 range errors (-3%, 3%). Similar to the VMAT plans, these position errors included isocenter position shifts in the six main directions and the eight diagonal directions of each octant in three-dimensional space.

Planned dose distributions

To explore differences between VMAT and IMPT plans, dose distributions for bladder, rectum and bowel cavity were evaluated. Planned dose parameters for the volumes receiving 15 Gy ($V_{15\text{Gy}}$), 30 Gy ($V_{30\text{Gy}}$) and 45 Gy ($V_{45\text{Gy}}$) were extracted [56,140]. Because we aim to treat with a full bladder to minimize bowel irradiation, only planned dose parameters of library plans representing the full bladder planning CT anatomy were evaluated.

Recalculated fraction doses

Using all weekly CTs, IGART and IGAPT treatments were simulated by selecting plans from the created plan libraries and recalculating fraction dose distributions based on our clinical applied strategy. First, image-guided patient alignment was simulated by registering CTs to the full bladder planning CT based on bony anatomy using only translations. Patient-specific ITV structures were projected on the registered CT and the ITV encompassing the pCTV was selected. Both VMAT and IMPT library plans corresponding to the selected ITV were recalculated on the registered CTs to obtain fraction dose distributions.

IGART and IGAPT fraction dose distributions were verified on target coverage and compared for OAR doses. Target coverage was assessed by calculating the CTV volume receiving at least 95% of the prescribed fraction dose ($V_{95\%}$). Differences in bladder, bowel cavity and rectum sparing were verified by calculating the mean (D_{mean}) and maximum ($D_{2\text{cc}}$) fraction dose and extracting fractionated substitutes of $V_{15\text{Gy}}$, $V_{30\text{Gy}}$ and $V_{45\text{Gy}}$ (i.e. $V_{15\text{Gy}}\text{-fx}$, $V_{30\text{Gy}}\text{-fx}$ and $V_{45\text{Gy}}\text{-fx}$). A fractionated substitute represents the volume receiving the corresponding fraction dose (i.e. the dose level divided by the number of fractions). Patient-specific DVHs were plotted and dose differences between IGART and IGAPT fractions were tested pairwise for significance using a non-parametric statistical test (Wilcoxon signed-rank test).

OAR toxicity

In addition to the analysis based on recalculated fraction dose distributions, differences in toxicity probabilities for bowel and rectum were estimated. Differences between the DVH parameter associated with overall rectum toxicity ($V_{30\text{Gy}}$) were derived [140]. For bowel, NTCP differences associated with at least grade 2 acute gastrointestinal toxicity were quantified using

$$NTCP = \frac{1}{1 + \left(\frac{V_{50}}{V_{45\text{Gy}}}\right)^k}$$

where $V_{45\text{Gy}}$ represents the volume (cm^3) receiving 45 Gy, $V_{50}=410 \text{ cm}^3$ and $k=3.2$ [141].

The toxicity-related DVH parameters (rectum $V_{30\text{Gy}}$, bowel cavity $V_{45\text{Gy}}$) were estimated by scaling patient-specific averages of rectum $V_{30\text{Gy}}$ -fx and bowel cavity $V_{45\text{Gy}}$ -fx with the prescribed number of fractions. Alternatively, CTs were registered deformable to the full bladder planning CT using the hybrid deformable registration algorithm implemented in RayStation [142]. Based on these registrations, fraction dose distributions were warped and weighted accumulated to derive total delivered dose distributions. Toxicity-related DVH parameter values were extracted and differences were tested pairwise using a non-parametric statistical test (Wilcoxon-signed rank test). The explanation and validation of the algorithm can be found in Appendix 5.A.

5.3 | Results

Per patient, plan libraries consisting of clinically acceptable VMAT and IMPT plans were created (Figure 5.2). Adequate ITV coverage ($D_{98\%} \geq 95\%$; $D_{2\%} \leq 107\%$) was found for all perturbed dose distributions after robustness evaluation and resulted in a total number of 58 robust library plans. Planned dose distributions indicated improvements in OAR sparing using IGAPT. The average planned $V_{15\text{Gy}}$, $V_{30\text{Gy}}$ and $V_{45\text{Gy}}$ decreased with 0.1%, 13.0% and 26.0%, 19.0%, 27.0% and 15.5%, and 43.2%, 26.9% and 10.7% for rectum, bladder and bowel cavity, respectively. Patient-specific DVHs of planned dose distributions are available online².

After dose recalculation on the weekly CTs, six simulated fractions (10.7%) from four different patients showed inadequate CTV coverage for both the IGART and IGAPT strategy. Due to substantial deviating anatomy compared to the pre-treatment derived full-range pITV, library plans were inappropriate and these fractions were excluded from further analysis. For the remaining fractions, adequate target coverage ($V_{95\%} > 98\%$) was obtained in 92% (96%) of the recalculated IGAPT (IGART) plans and results on planned and recalculated target dose ($D_{98\%}$, $D_{2\%}$) are presented (Figure 5.3). Although two (four) fractions resulted in CTV $V_{95\%} < 98\%$ for the IGART (IGAPT) strategy while the IGAPT (IGART) strategy resulted in CTV $V_{95\%} > 98\%$, the average CTV coverage per patient was adequate for both strategies.

² <http://www.tandfonline.com/doi/suppl/10.3109/0284186X.2016.1139179>

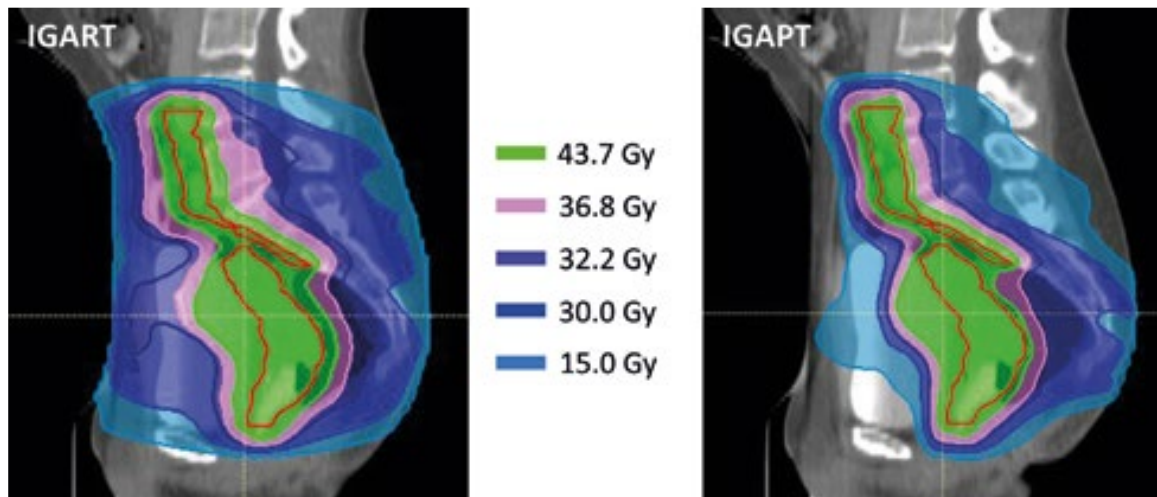


Figure 5.2 | Sagittal view of color wash map examples of dose distributions are shown for the IGART strategy (left) and the IGAPT strategy (right). Both dose distributions indicated adequate CTV (red) coverage while large differences in low and medium dose to surrounding healthy tissue are observed.

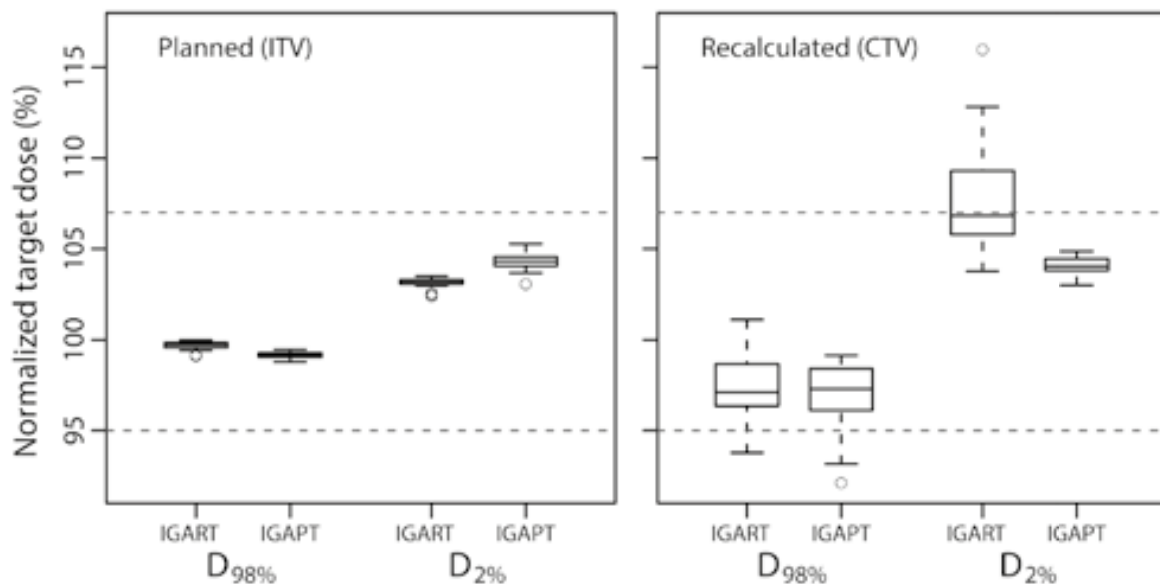


Figure 5.3 | For the planned dose distributions based on the ITV (left) and the recalculated dose distribution based on the CTV (right), boxplots of target dose parameters over all patients are shown as percentage of the prescribed dose for both the IGART and the IGAPT strategy. Boxes represent upper and lower quartiles (IQR), the band inside the box the median value and the whiskers the highest (lowest) value within 1.5 IQR of the upper (lower) quartile.

The simulated fractions indicated OAR dose reductions for $V_{15\text{Gy}}\text{-fx}$, $V_{30\text{Gy}}\text{-fx}$ and $V_{45\text{Gy}}\text{-fx}$, similar to the OAR dose reductions represented by the planned dose distributions. As an example, Figure 5.4 shows DVHs of recalculated fraction dose distributions for two typical patients. Patient-specific DVHs of recalculated fraction dose distributions are available online². All DVH parameters, except

rectum $V_{45\text{Gy}}\text{-fx}$, showed a relative improvement in OAR sparing when using IGAPT. Also, both D_{mean} and $V_{30\text{Gy}}\text{-fx}$ for bladder, rectum and bowel cavity decreased significantly (Figure 5.5). Table 5.3 presents the mean dosimetric parameter values for the OAR evaluations and the absolute and relative differences between IGART and IGAPT.

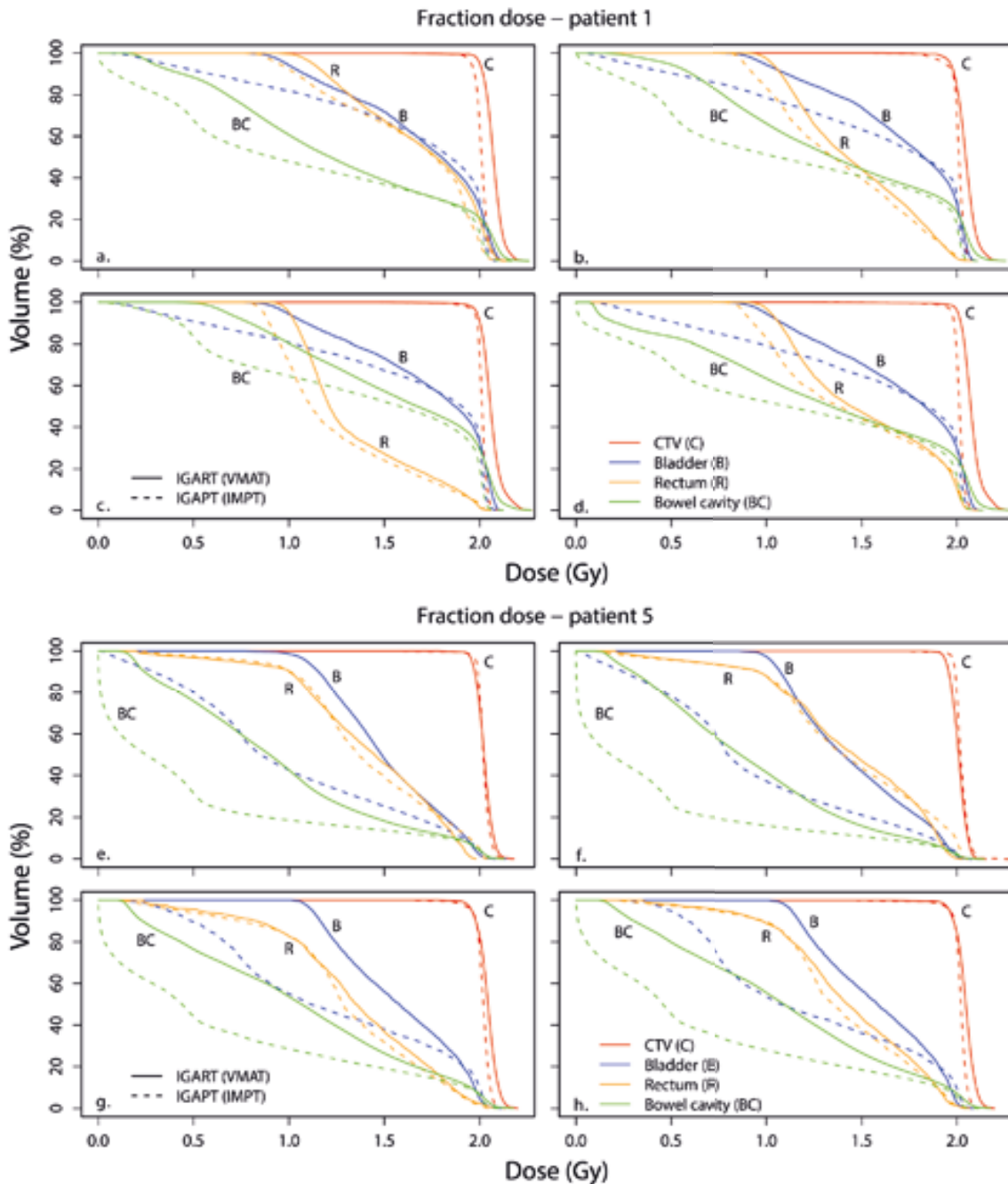


Figure 5.4 | For patient 1 (a-d) and patient 5 (e-h), DVHs of recalculated fraction dose distributions are shown for target and OARs based on VMAT plans for the IGART strategy (solid lines) and IMPT plans for the IGAPT strategy (dotted lines). The intersection of the 2 solid black lines indicates $V_{95\%}=98\%$. For one fraction of patient 1 (b), IGAPT resulted in inadequate CTV coverage while CTV coverage using IGART was adequate.

The scaled averages of DVH parameters indicated a reduction in rectum $V_{30\text{Gy}}$ of 8% for IGAPT (average, 69%) compared to IGART (average, 77%). Also, a decrease in NTCP for bowel of 0.07 was estimated for IGAPT (average, 0.43) compared to IGART (average, 0.50). Dose accumulation based on deformable registration resulted in an average rectum $V_{30\text{Gy}}$ difference of 7% between IGART (average, 81%) and IGAPT (average, 74%). For bowel, the NTCP decreased on average 0.15 when using IGAPT (average, 0.18) instead of IGART (average, 0.33). Moreover, IGAPT resulted in significant improvements ($p < 0.01$) for rectum $V_{30\text{Gy}}$ and bowel NTCP. However, two (one) patients showed a limited increase in rectum $V_{30\text{Gy}}$ (bowel NTCP) for IGAPT compared to IGART.

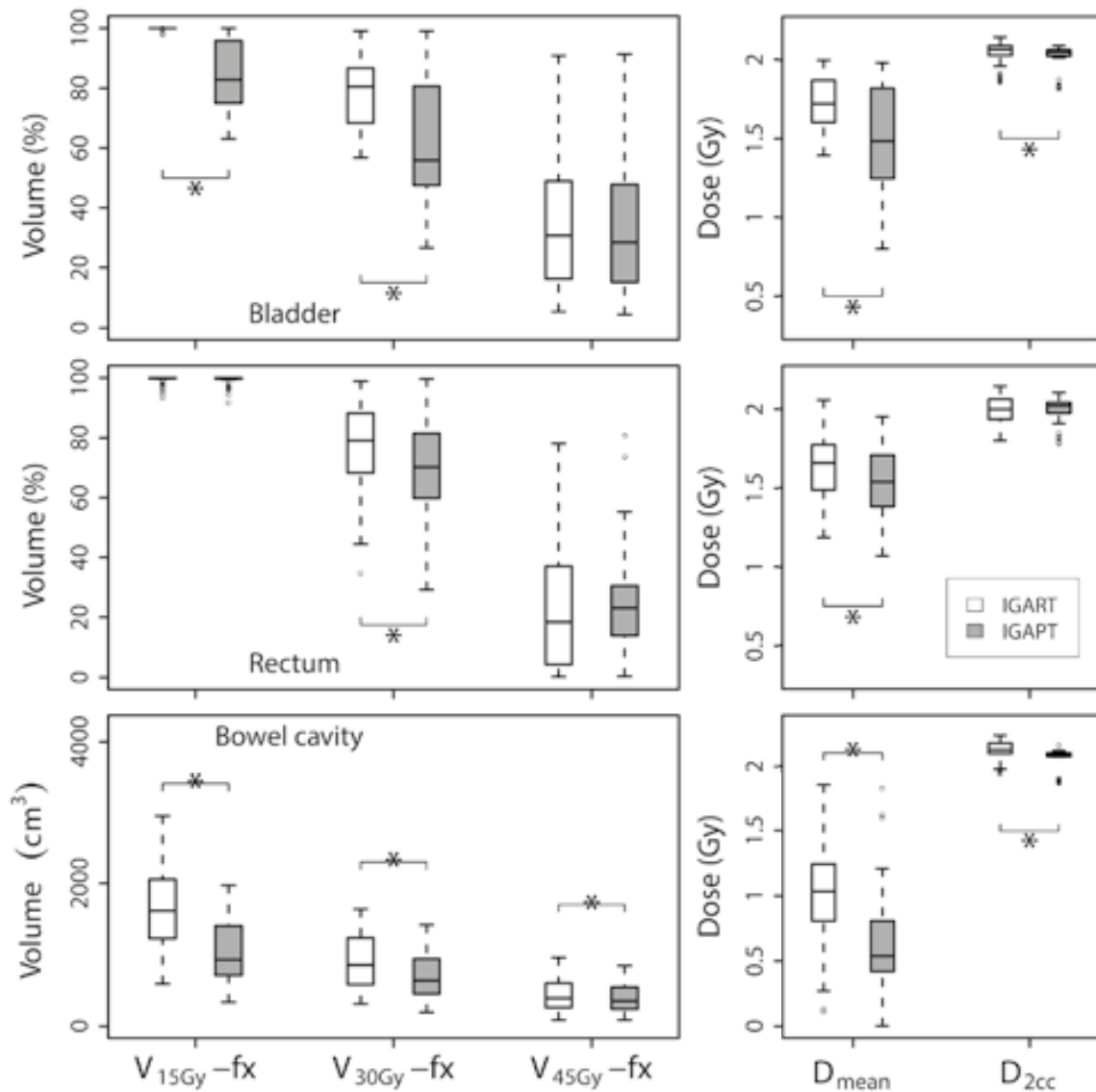


Figure 5.5 | For bladder (upper), rectum (middle) and bowel cavity (lower), boxplots of fraction DVH parameters over all analyzed fractions of all patients are shown. Boxes represent upper and lower quartiles (IQR), the band inside the box the median value and the whiskers the highest (lowest) value within 1.5 IQR of the upper (lower) quartile. Horizontal lines including an asterisk indicate statistical significant difference ($p < 0.01$) based on a paired non-parametric statistical test.

Table 5.3 | Comparison of the mean dosimetric parameters for the recalculated fractions of all patients.

	IGART	IGAPT	Absolute difference (IGART – IGAPT)	Relative difference (%)	<i>p</i> -Value
Bladder					
$V_{15\text{Gy}}\text{-fx}$ (%)	99.9	84	15.8	15.9	<.001
$V_{30\text{Gy}}\text{-fx}$ (%)	78.2	62.9	15.4	21.1	<.001
$V_{45\text{Gy}}\text{-fx}$ (%)	36.3	34.7	1.7	3.3	0.08
D_{mean} (Gy)	1.7	1.5	0.2	13	<.001
$D_{2\text{cc}}$ (Gy)	2.0	2.0	0.0	1.4	<.001
Rectum					
$V_{15\text{Gy}}\text{-fx}$ (%)	99.3	99.2	0.1	0.1	0.3
$V_{30\text{Gy}}\text{-fx}$ (%)	77.6	70.3	7.3	10.0	<.001
$V_{45\text{Gy}}\text{-fx}$ (%)	23.6	24.5	-0.9	-12.7	0.46
D_{mean} (Gy)	1.6	1.5	0.1	5.3	<.001
$D_{2\text{cc}}$ (Gy)	2.0	2.0	0.0	0.0	0.91
Bowel cavity					
$V_{15\text{Gy}}\text{-fx}$ (cm ³)	1673.1	1012.8	660.3	37.8	<.001
$V_{30\text{Gy}}\text{-fx}$ (cm ³)	887.2	693.8	193.5	22.4	<.001
$V_{45\text{Gy}}\text{-fx}$ (cm ³)	428.0	387.0	41.1	7.8	<.001
D_{mean} (Gy)	1.0	0.6	0.4	45.0	<.001
$D_{2\text{cc}}$ (Gy)	2.1	2.1	0.1	3.0	<.001

Abbreviations: IGART = image-guided adaptive radiation therapy; IGAPT = image-guided adaptive proton therapy; fx = fractionated substitute.

5.4 | Discussion

In this study, we investigated the feasibility and potential dosimetric advantages of adaptive proton therapy compared to adaptive photon therapy in cervical cancer. Using a plan-library based plan-of-the-day image-guided adaptive strategy to compensate for anatomical interfraction changes, IGART and IGAPT treatments were simulated using weekly CTs and compared for target coverage and OAR dose. Our study is the first to demonstrate the potential benefit of image-guided adaptive proton therapy in cervical cancer including a dosimetric analysis based on weekly CTs. Compared to photon-based IGART, IGAPT maintains adequate target coverage while significant dose reductions can be achieved for bladder, bowel cavity and rectum, which results in decreased toxicity.

Unlike previously reported studies on proton therapy in cervical cancer [69-71,123], our analysis included treatment simulations by recalculating dose distributions using additional imaging obtained during treatment. To anticipate on anatomical changes during the treatment

course and prevent incorrect dose delivery, we combined proton therapy with a state-of-the-art adaptive strategy. Consequently, our recalculated dose distributions are more representative in terms of target coverage and OAR sparing compared to the use of only planned proton dose distributions.

Besides the recalculation of dose distributions, the highly recommended robust optimization for proton therapy planning was applied using reported uncertainty values instead of using the photon-based PTV concept based on population-based margins [24,138]. However, uncertainty values reflecting the optimal trade-off between target coverage robustness and OAR sparing need to be derived. To compare IGART and IGAPT fairly, also VMAT plans were robustly optimized using reported uncertainty values thereby eliminating the influence of different optimization techniques. Consequently, IGART results derived in this study do not directly represent results of our clinically applied PTV-based IGART treatments. To complete the comparison between IGART and IGAPT, additional research is needed to investigate the dosimetric advantage of IGAPT compared to our clinical IGART results.

Except for the robust optimization, the applied adaptive strategy in this study is similar to our clinically implemented adaptive strategy for cervical cancer RT. Prior to treatment, the full-range pITV was derived based on two planning CTs with extreme bladder volumes and interpolated to obtain pITV subranges. The number of pITVs generated is based on our clinical experience and the pre-treatment predicted full-range pITV was sufficient for almost all included patients. However, 10.7% of all fractions showed substantial deviation from the pre-treatment derived full-range pITV which resulted in inappropriate library plans. Since additional shifts after bony registration are not permitted to ensure lymph node coverage, treatment fractions will be postponed in clinical practice and justified the exclusion of this limited amount of fractions from our analysis. Even when this percentage increases, the use of a motion-robust backup plan (i.e. single field uniform dose plan to the full-range ITV, including robust optimization using larger uncertainty values) can be considered.

Next to interfraction motion, intrafraction organ motion during cervical cancer radiation therapy can be considerable and might affect dose delivery [74]. Besides potentially prolonged delivery times, IGAPT is more sensitive to uncertainties compared to IGART and intrafraction motion should be taken into account. In this study, we anticipated on possible intrafraction motion by robust optimization using appropriate uncertainty values. Moreover, the use of ITVs in our proposed adaptive strategy already compensated for possible intrafraction target motion induced by intrafraction bladder filling. Hence, the combination of ITVs with robust optimization is assumed to limit dosimetric consequences of intrafraction motion.

Similar to our current clinical workflow, all library plans were optimized using the full bladder planning CT. Preferably, plan optimization would be performed using the CT representing the corresponding anatomy. However, since multiple library plans were created corresponding to targets obtained by interpolation, available planning CTs do not necessarily represent associated anatomy for all target volumes.

Similar to the plan selection procedure applied clinically, the library plan best fitting the target shape and position as seen on CT was selected visually after bony registration. In our study, plan selection was relatively easy since only CTs were used. CBCT-based plan selection is more challenging due to limited soft-tissue contrast, resulting in an additional observer variation. To minimize the effect of this variation, plan selection based on automatic organ segmentation could be applied [75]. However, disturbed CBCT quality could hinder automatic organ segmentation and still require manual selection. Alternatively, dose-guided plan selection could be beneficial and can be applied when online recalculation of library plans based on pre-fraction imaging will become available [143].

Although cervical cancer irradiation is generally delivered in 23 or 28 fractions, we only used a limited number of weekly CTs per patient to simulate adaptive treatments. Consequently, the complete range of anatomical deformations occurring during the course of treatment are not necessarily included. Even though the included anatomical changes can influence observed dose differences due to their weighted contribution, this influence is assumed to be limited due to the substantial number of included patients. To completely eliminate these possible overestimations or underestimations of dosimetric differences, daily anatomical variations preferably based on an increased number of patients need to be included. However, daily CBCT images are not directly suitable for dose calculations.

Our dosimetric analysis is mainly based on DVHs of recalculated fraction dose distributions, from which parameter values were extracted. DVH parameter differences between recalculated IGART and IGAPT fractions were analyzed and statistical tests were applied pairwise to allow different fractionation schemes. In addition to the analysis based on fraction DVH parameters, reductions in toxicity probabilities for rectum and bowel were estimated based on DVH parameters representing the complete treatment course. Because no spatial information is present in fraction DVHs, the scaled average fraction DVH parameter approximation not necessarily represents reliably accumulated OAR parameter values. Therefore, DVH parameters were also derived based on dose accumulation after deformable image registration. For rectum V_{30Gy} , both methods resulted in similar parameter values while an improvement for bowel V_{45Gy} was observed when using the dose accumulation method.

Although the deformable registration algorithm was validated previously for pelvic registrations [142], we validated our registrations by visual inspection and OAR similarity quantification to ensure plausible dose warping. However, an extensive validation of the complete anatomical correctness and the influence of possible incorrectness on dose accumulation is still an important challenge in RT [144] and beyond the scope of this study.

According to QUANTEC recommendations, differences in NTCP for grade 2 acute gastrointestinal toxicity were quantified using the associated DVH parameter (bowel V_{45Gy}) [141]. However, the recommended lowest toxicity thresholds for rectum ($V_{50Gy} < 50\%$) and bladder ($V_{65Gy} < 50\%$) were in our study never reached. To differentiate between IGAPT and IGART, the reported DVH parameter associated with overall rectum toxicity (V_{30Gy}) was used [140].

Even though the application of IGAPT in cervical cancer has been demonstrated, additional steps will have to be taken before implementing this technique clinically. Daily pre-fraction imaging, preferably using MRI or CT, will be required for plan selection. In addition, appropriate clinical protocols regarding plan selection need to be developed.

5.5 | Conclusion

Our study demonstrates the feasibility of adaptive proton therapy in cervical cancer. Compared to photon-based IGART, simulated IGAPT treatments result in adequate target coverage while the OAR dose decreases significantly. In addition, our results indicate toxicity probability reductions, but further analysis is needed to determine clinical outcome in terms of toxicity.

Appendix 5.A

In this study, weekly acquired repeat CTs were deformable registered to the full bladder planning CT using the hybrid deformable registration algorithm implemented in RayStation (version 4.4, RaySearch Laboratories AB, Stockholm, Sweden). This algorithm combines image information (i.e. image intensities) with anatomical information as provided by delineated structures [142]. The objective function is a linear combination of four nonlinear terms: 1) image similarity term (to maintain image similarity), 2) grid regularization term (to keep the image grid smooth and invertible), 3) a shape based regularization term (to keep the deformation anatomically reasonable when regions of interest are present) and 4) a penalty term when controlling structures are used (to deform the selected structure in the reference image to the corresponding structure in the target image).

The deformable registrations performed between the repeat CTs and the full bladder planning CT were guided by contoured structures present in both image sets. By providing all anatomical information available in term of contoured structures, the optimization function is steered towards anatomical plausible registrations. For our analysis, the delineated bladder, rectum, pCTV, bowel cavity, left hip and right hip structures were included. Registration results were first visually verified by overlying the registered image sets. Due to the absence of a set of unique corresponding landmark for both image sets to validate deformable registrations, two commonly used similarity measures were used for validation [75,84,144]. First, the similarity of registered structures was quantified using the Dice similarity coefficient (DSC) for the structures of interest. Additionally, the surface distance error (SDE), i.e. the mean of distances between registered corresponding structures, was calculated to confirm structure similarity.

For all patients, the obtained deformable registrations between the full bladder planning CT and repeat CTs were considered accurate after visual inspection. Also, similarity between inspected structures after deformable registration was sufficient in terms of DSC and SDE. Table 5.A.1 represents average results of applied deformable registrations per patient for DSC as well as SDE.

Table 5.A.1 | Results of deformable image registration per patient, represented by the mean DSC and SDE for contoured structures.

Patient	DSC (-)						SDE (cm)					
	bladder	rectum	bowel cavity	pCTV	left hip	right hip	bladder	rectum	bowel cavity	pCTV	left hip	right hip
1	0.96	0.93	0.94	0.92	0.98	0.98	0.05	0.10	0.15	0.17	0.01	0.01
2	0.88	0.91	0.88	0.84	0.98	0.98	0.15	0.17	0.27	0.19	0.02	0.02
3	0.91	0.94	0.90	0.91	0.98	0.98	0.11	0.08	0.24	0.16	0.02	0.02
4	0.91	0.92	0.89	0.89	0.95	0.96	0.14	0.12	0.46	0.19	0.05	0.04
5	0.87	0.91	0.93	0.87	0.98	0.98	0.18	0.08	0.26	0.13	0.02	0.02
6	0.82	0.90	0.89	0.91	0.97	0.97	0.22	0.16	0.30	0.23	0.03	0.03
7	0.97	0.93	0.93	0.94	0.98	0.98	0.03	0.14	0.23	0.06	0.02	0.02
8	0.96	0.89	0.97	0.97	0.98	0.98	0.04	0.34	0.12	0.05	0.01	0.02
9	0.69	0.73	0.83	0.81	0.95	0.96	0.23	0.30	0.58	0.37	0.06	0.05
10	0.98	0.92	0.96	0.91	0.98	0.98	0.03	0.12	0.20	0.13	0.02	0.02
11	0.96	0.93	0.88	0.93	0.98	0.98	0.04	0.12	0.67	0.13	0.02	0.02
12	0.92	0.93	0.89	0.90	0.97	0.98	0.10	0.09	0.28	0.14	0.03	0.03

Abbreviations: DSC = Dice similarity coefficient; SDE = surface distance error; pCTV = primary clinical target volume.